J Membrane Biol (2014) 247:501–514
DOI 10.1007/s00232-014-9660-1

Biomineralization Studies on Cellulose Membrane Exposed to Biological Fluids of *Anodonta cygnea*

Anabela Lopes · Manuel Lopes-Lima · Jorge Ferreira · Sandra Araújo · Mariana Hinzmann · José Oliveira · António Rocha · Bernardo Domingues · Iulius Bobos · Jorge Machado

Received: 3 October 2013 / Accepted: 17 March 2014 / Published online: 8 April 2014

Abstract The present work proposes to analyse the results obtained under in vitro conditions where cellulose artificial membranes were incubated with biological fluids from the freshwater bivalve *Anodonta cygnea*. The membranes were mounted between two half 'Ussing chambers' with different composition solutions in order to simulate epithelial surfaces separating organic fluid compartments. The membrane surfaces were submitted to two synthetic calcium and phosphate solutions on opposite sides, at pH 6.0, 7.0 or 9.0 during a period of 6 hours. Additional assays were accomplished mixing these solutions with haemolymph or extrapallial fluid from *A. cygnea,* only on the calcium side. A selective ion movement, mainly dependent on the membrane pore size and/or cationic affinity, occurred with higher permeability for calcium ions to the opposite phosphate chamber supported by calcium diffusion forces across the cellulose membrane. In general, this promoted a more intense mineral precipitation on the phosphate membrane surface. A strong deposition of calcium phosphate mineral was observed at pH 9.0 as a primary layer with a homogeneous microstructure, being totally absent at pH 6.0. The membrane showed an additional crystal phase at pH 7.0 exhibiting a very particular hexagonal or *cuttlebone* shape, mainly on the phosphate surface. When organic fluids of *A. cygnea* were included, these crystal forms presented a high tendency to aggregate under *rosaceous* shapes, also predominantly in the phosphate side. The cellulose membrane was permeable to small organic molecules that diffused from the calcium towards the phosphate side. In the calcium side, very few similar crystals were observed. The presence of organic matrix from *A. cygnea* fluids induced a preliminary apatite–brushite crystal polymorphism. So, the present results suggest that cellulose membranes can be used as surrogates of biological epithelia with preferential ionic diffusion from the calcium to the phosphate side where the main mineral precipitation events occurred. Additionally, the organic fluids from freshwater bivalves should be also thoroughly researched in the applied biomedical field, as mineral nucleators and crystal modulators on biosynthetic systems.

Keywords Cellulose membranes · Biomineralization · *Anodonta cygnea* · Biological fluids

A. Lopes · M. Lopes-Lima · S. Araújo · M. Hinzmann · A. Rocha · B. Domingues · J. Machado (✉)
ICBAS - Instituto de Ciências Biomédicas Abel Salazar, Laboratório de Fisiologia Aplicada, Rua de Jorge Viterbo Ferreira No. 228, 4050-313 Porto, Portugal
e-mail: jmachado@icbas.up.pt

A. Lopes · M. Lopes-Lima · M. Hinzmann · B. Domingues · J. Machado
CIIMAR - Centro de Investigação Marítima e Ambiental, Rua dos Bragas 289, 4050-123 Porto, Portugal

J. Ferreira
INETI - Instituto Nacional de Engenharia, Tecnologia e Inovação, I.P, Rua da Amieira, 4466-956 S. Mamede de Infesta, Portugal

J. Oliveira
CHP-Centro Hospitalar do Porto, Serviço Química Clínica (HGSA), Largo Prof. Abel Salazar, 4099-001 Porto, Portugal

I. Bobos
FCUP - Faculdade de Ciências da Universidade do Porto, Departamento de Geociências, Rua Campo Alegre 687, 4169-007 Porto, Portugal

Introduction

Biomineralization is the process by which organisms produce minerals from biological solutions for their own functional requirements (Carter 1990; Lopez et al. 1992;

Janis 1995; Kroger et al. 2000; Javaux et al. 2001; Vekilov and Chernov 2002; De Yoreo and Vekilov 2003). Several examples demonstrated that organisms are able to control the location and crystallographic orientation, the shape of the growing crystallites and even the phase of the resulting materials during the nucleation process (Falini et al. 1995; Belcher et al. 1996; Mount et al. 2004). Examples of biological calcite and aragonite models where this phenomenon occur showed single shaped crystals with intricate crystal composites and regular crystal laminates. In these models, calcite is generally a more stable form of calcium carbonate than aragonite, at least in standard conditions (Checa et al. 2006; Lopes-Lima et al. 2010). Depending on the presence of additional compounds in solution, it is possible to obtain particular crystal changes and combinations e.g. carbonated hydroxyapatite, when both calcium carbonate and phosphate may co-occur (Lopes et al. 2010). In summary, the microstructure and even the crystal polymorphism may depend on the physical–chemical conditions of the biomineralization microenvironment (Falini et al. 1995; Belcher et al. 1996; Mount et al. 2004; Checa et al. 2006; Takeuchi et al. 2008).

It is commonly understood that, in addition to be genetically directed (Addadi and Weiner 1992), the organic matrix from molluscan shells regulates the crystal formation and growth, theoretically through an ionotropic or stereochemical mechanism (Takeuchi et al. 2008). According to studies by J. Machado research team at the University of Porto, the freshwater mussel *Anodonta cygnea* is an adequate model to carry out 'in vitro' assays on biomineralization processes due to a facilitated access into two compartments where abundant and specific organic matrixes compose the biological media: the haemolymph and the extrapallial fluid. Here, specific molecules, such as proteins or smaller fractions (e.g. peptides), glycosaminoglycans (GAGs) and hexosamines (chitin) from the haemolymph can be deeply involved on microspherules (calcium phosphate and carbonate concretions) mineralization, while in the extrapallial fluid, similar organic molecules support shell calcification under calcium carbonate nacre (Moura et al. 2000, 2001, 2003a; Lopes-Lima et al. 2005, 2010).

On the other hand, recent works on natural polymers and biomembranes revealed extensive and important theoretical and applied concepts on the biomedical field (Colton et al. 1971, Farrell and Babb 1973; Leoni et al. 2002; Nielsch et al. 2002; Darder et al. 2006; Ehrlich et al. 2006; Santos et al. 2007; Mano et al. 2007, 2008; Silva et al. 2008).

The affinity or adsorptive properties attributed to the separation membranes technology based on functional groups in the membrane surface have been largely studied in several applications such as in the biomedical, biochemical and environmental fields (Büyüktuncel et al. 2001; Avramescu et al. 2002; Chen et al. 2004; Nunes and Peinemann 2006; Albrecht et al. 2007; Koyuncu et al. 2008; Ventura et al. 2008; Saufi and Fee 2009; Lay et al. 2010). Conventional adsorptive membranes were usually prepared by surface modification (Moura et al. 1999, 2000; Lopes-Lima et al. 2010). However, more recently membrane surface modifications based on polymers or composites addition with specific functional groups have been accomplished (Liu and Bai 2005, 2006; Han et al. 2007; Karppi et al. 2010).

An evaluation of some recent molecular scale assays is here accomplished to reveal new insights into the formation and control of crystal growth by organic and inorganic molecules, under particular conditions. The present work proposes to analyse results obtained under semi-synthetic conditions where artificial membranes were bathed with both biological fluids from *A. cygnea*.

In mussels, organic and inorganic molecules function selectively as active inducers and modulators of crystal formation under calcitic or aragonitic systems, but when complemented artificially with calcium carbonate and phosphate artificial solutions under in vitro conditions distinct minerals such as hydroxyapatite may occur (Lopes et al. 2010). Simulating epithelial electrophysiology assays, synthetic membranes can be mounted between two half 'Ussing Chambers' in order to mimic both surfaces of an epithelial membrane separating two biological compartments (Lopes et al. 2010).

Dialysis membranes should be good candidates for biomineralization studies since it can exhibit dynamic phenomena on its surface similar to physiological membrane processes. As an example, Childress and Elimelech (1996) investigated the chemical composition effect of a solution on the surface charge properties of various commercial reverse osmosis and nanofiltration membranes. They observed that humic substances and surfactants readily adsorb to the membrane surface and clearly influence the membrane surface charge giving adequate properties.

Beyond the liquid solute composition, it is also relevant to evaluate the adequate pH for a specific synthetic membrane in order to observe that an appropriate interface is well preserved and that the fibres are not degraded in the process (Thygesen et al. 2005; Xiong et al. 2010). A reduction in the interface binding efficiency leads to a lower epitaxial process on the biomineral deposition. It is therefore, important to determine the experimental conditions (e.g. pH) that the fibres can tolerate without severe degradation. Usually, the effect of acidic conditions on the interface, strength and cristallinity of chitosan or cellulose fibres is the main factor to be controlled (Thygesen et al. 2007; Lopes et al. 2010).

In the present work, the study was accomplished on a commercial semi-permeable membrane of synthetic cellulose which is usually applied on dialysis processes. This selective

process constitutes an interesting property for biomineralization studies since they can partially simulate biological membranes. Additionally, these membranes are easy to synthesize and use, and are relatively inexpensive. One relevant aspect to be considered is the cellulose membrane selectivity which is dependent on the pore size (Singh et al. 1998; Mehta and Zydney 2005). So, if the size of a solute, highly correlated with molecular weight, approaches or exceeds the size of pores membrane (MWCO) its passage will be partially or completely prevented (Ren et al. 2006). Restriction to molecular diffusion is a function of pore radius and molecular radius according to experiments with cellulose membranes by Renkin (1954), Farrell and Babb (1973) and Mahendran et al. (2004), as well as to the theory of membrane pore permeability proposed by Pappenheimer et al. (1953).

On this view, our aim was to gain further knowledge about the basic principles of biomineralization and to evaluate the influence of bivalve biological fluids, which are determinant on in vivo biomineralization events. The study was accomplished using 'Ussing chambers' in vitro assays with cellulose membranes in order to understand the influence of artificial solutions composition on the deposited mineral phases with or without biological fluids of *A. cygnea* at different pH conditions.

Experimental

Cellulose Membrane

The cellulose membrane (Membrane Filtration Products, Inc. #2550-40) used was a dialysis membrane with a 25 KDa of pore size. The membrane treatment was performed as in the manufacturer instructions by soaking the membrane pieces with distilled water for 10 min. This membrane presents an electrical resistance which become, in general, very selective to ions and molecules diffusion. Reid and Breton (1959) suggested that cellulose acetate exhibits a clear semipermeability property. It is due to this situation that across the membrane strong electrolytes diffuse very slowly compared to the rate of water diffusion. They suggested that only ions and molecules that can combine with the membrane through hydrogen bonding and can fit into the bound water structure are presumed to be transported across the membrane by alignment of hydrogen bonds with the membrane. Additionally, temporal conformation change took place on the water bound to the cellulose surface occurred as a result of a stabilized hydration layer (Ohata et al. 2004).

Biological Sample Collection

Freshwater bivalves (*A. cygnea*) were collected from the bottom of Barrinha de Mira lagoon (Coimbra, Portugal). The animals were kept in the laboratory on dechlorinated and aerated water for a minimum of 24 h before fluid (haemolymph and extrapallial fluid) extraction. For the fluids sampling, the animals were considered healthy if they showed active ventilation and powerful valve closing or water ejection upon disturbance. For each experiment, approximately 5 ml of haemolymph and 5 ml of extrapallial fluid were extracted from two animals with a needle syringe delicately inserted in the interepithelial of the mantle and in the shell compartment, respectively. Each fluid was then centrifuged at 4000 rpm, 5 min. (Kubota KR-20000T, Rotor RA-3R) to remove cellular debris. Subsequently, the supernatant collected in order to be used in the following experimental procedures.

Experimental Scheme

The experimental scheme was similar to that already described in Lopes et al. (2010). The main difference from the previous study was in the nature of the membrane used.

It should be emphasized that the calcium chloride (20 mM) and sodium phosphate (20 mM) synthetic solutions have initial different pHs. So, these solutions were adequately titrated with HCl, citric, succinic acids (1 M) or with NaOH (1 M) in order to reach pH 6.0, 7.0 or 9.0. Experimental procedures used the same parameters, such as temperature, bathing solution volume and number of replicates in all assays.

In these experiments, 'Ussing chambers' which were separated by a cellulose membrane in two compartments were filled with artificial solutions previously set at pH 6.0, 7.0 and 9.0. One chamber was filled with 4 ml of sodium phosphate (20 mM) (left chamber) and the other with 4 ml of calcium chloride (20 mM) (right chamber) (Diagram 1). Using this configuration, three experimental groups were set for only the synthetic solutions adjusted to acidic and neutral pH values (6.0 and 7.0), each with three distinct organic acids (HCl, succinic and citric) and one experimental group at pH 9.0. Two additional experimental groups were set for each of the previous situations where haemolymph or extrapallial fluid was added only to the calcium chamber. In these two last groups, the calcium content was adjusted to 20 mM in the calcium chamber (Lopes et al. 2010).

Fluid Composition Analysis

For all experiments (see Diagram 1), each fluid composition was analyzed using six fluid sample replicas collected at time zero (control time) and after a period of 6 h of bathing (experimental time).

The final concentration of ionic calcium and phosphate, per each acidified pH 6.0 and 7.0 solutions, resulted from the average of 6 assays using three distinct acids (HCl, succinic and citric acids solutions) ($n = 18$). For each of the

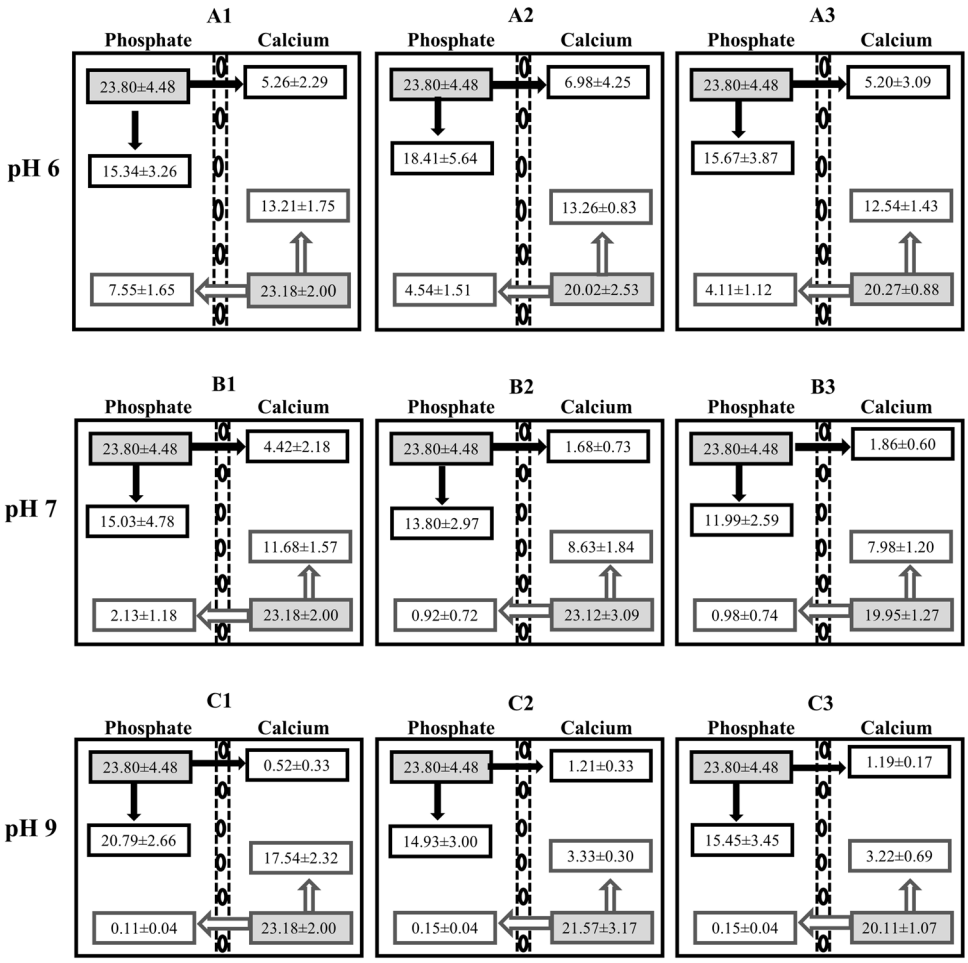

Diagram 1 Variations of phosphate and calcium contents in Ussing chambers after 6.0 h after at: **a** pH 6.0; **b** 7.0 and **c** 9.0 without (*1*) or with haemolymph (*2*) or extrapallial fluid (*3*) bathing the cellulose membranes. In each experimental set (*box*) for pH 6.0 and 7.0 ($n = 54$) and pH 9.0 ($n = 18$). (*Grey cells*) Original calcium and phosphate contents at time zero in the respective addition sides; (*arrows*) calcium and phosphate ionic diffusion and respective final contents after 6.0 h bathing in the original and opposite sides

previous situations, three fluid sample replicas were collected and analyzed accomplishing a total of 54 ($n = 18 \times 3$) measurements per ion. On the other hand, the final values of same elements in the basic solutions titrated with NaOH to pH 9.0, and the results from the average of six assays with three analytic replicas giving a total number of 18 $n = (6 \times 3)$ measurements per compound. Concerning the experiments with the addition of biological haemolymph and extrapallial fluids at pH values 6.0 and 7.0, the same amount of measurements was carried out for calcium and phosphate ions, proteins, lipids and GAGs, also with a total of 54 for each fluid. In a similar way for the experiments at pH 9.0, 18 measurements were also carried out for the same elements and compounds (Diagram 1).

Calcium and Phosphate Analysis

The Ca^{2+} ion contents were measured in a Cobas Integra system (Roche Diagnostics) at Hospital Geral Santo António (Porto, Portugal). The PO_4^{3-} contents were measured with PiBlueTM Phosphate Assay Kit (Bioassay Systems).

Protein, Lipids and GAGs Analysis

All organic molecules were quantified by colorimetric assays as described by Lopes et al. (2010) with the exception of GAGs which were quantified according to Whiteman (1973). The organic measurements were exclusively considered in the calcium chamber since the opposite phosphate chamber did not show detectable levels with the present methods.

Scanning Electron Microscopy (SEM) Imaging

Cellulose membrane pieces (2–3 replicas from each treatment in a total of 42 samples) were selected from the most representative assays of the different experimental sets and prepared for respective SEM imaging analyses on both surfaces of the membrane. For this, membrane pieces were gold-coated (FINECOAT Ion sputter JFC1100) and glued to aluminium stubs for SEM observations using JEOL JSM35C scanning electron microscope (SEM) operated at 10 Kv.

Fourier Transform Infrared Spectroscopy (FTIR) and X-Ray Diffraction (XRD)

Selected samples (18) of the most representative assays were analyzed by attenuated transmission reflectance ATR-infrared (IR) Bruker Equinox spectrometer coupled at a Bruker microscope that collected the IR beam with Cassegrain objectives. Analysis of films deposited on a CaF_2 disc was carried out by transmission, using a circular diaphragm with a 60 mm diameter aperture. Each spectrum was processed using the OPUS program (® Bruker). Spectra of atmospheric CO_2 and H_2O were recorded independently for subtraction purposes.

The XRD spectra were performed on a Panalytical Xpert MPD with a Cu vial.

Statistical Analyses

For all experiments, the differences in inorganic and organic contents were established between the mean values of samples collected at control period (time zero) and the mean values of the samples collected 6 h after bathing. These differences were tested for statistical significance by simple Paired t-tests using SPSS version 12.0 for Windows (SPSS Inc., Chicago, Illinois, USA). The significance level for all statistical analyses was set at 0.05

Results

In the present research, some specific functional aspects of the cellulose membrane were clearly observed, when bathed by specific media as described herein. In general, the results proved that in all assays, except at pH 6.0 (Fig. 1a), the cellulose membrane exhibited excellent inductor and adhesive properties for mineral deposits, confirmed by SEM, FTIR and X-ray analyses (Figs. 1, 2, 3, 4, 5, 6), being more effective in the phosphate side. Both membrane surfaces presented a wide homogeneous layer of calcium phosphate, as a primary mineral phase mainly at pH 9.0 (Fig. 1d). This homogeneous base, showed by SEM magnification a peculiar and uniform deposit as a '*foliated microstructure*' covering the whole membrane. This occurred when the membrane was bathed with succinic solution plus or without biological fluids (Fig. 1c). Over this '*foliated*' homogeneous layer, singular calcium phosphate crystals were detected when bathed by pH 7.0 solutions, mainly in the phosphate membrane surface.

Calcium and Phosphate Analyses

The results of ionic contents after 6 h of bathing (Diagram 1) concerning the different assays at pH 6.0, 7.0, 9.0 inform about the calcium and phosphate variations occurring in simple synthetic solutions (A1, B1, C1) or combined with haemolymph (A2, B2, C2) or extrapallial fluid (A3, B3, C3). In general, the results show a significant reduction ($p < 0.05$) on the calcium and phosphate concentrations from the initial solutions, except at pH 6.0 (Diagram 1a). In fact, at pH 7.0 and 9.0, significant losses ($p < 0.05$) of calcium and phosphate ions were verified during experimental period (Diagram 1b, c). These ionic decreases were more intense mainly at pH 9.0 and when the biological fluids were included and may correspond to the ion amounts used on the calcium phosphate precipitation in the both cellulose membranes surfaces. On the contrary, at pH 6.0, both calcium and phosphate ions presented significant diffusion movements ($p < 0.05$), but the ionic concentration of the initial and final solutions (sum from both sides) was very similar in concordance with the total absence of mineral deposits in both surfaces (Diagram 1a). All these aspects reveal a very specific behaviour of cellulose membrane in Ussing chambers, which seems to reproduce a selective ion and macromolecule permeability similar to what happens in biological epithelia.

When haemopymph or extrapallial fluids are used, the respective experimental data (Diagram 1b, c) still show that significant and stronger decreases of calcium and phosphate concentrations occurred corresponding to larger mineral precipitation, again more intense in the phosphate chamber. On the other hand, this mineral deposition also depends on the experimental pH, being clearly higher at alkaline pH, which is confirmed by stronger reductions of respective ions in this condition.

As a summary, mainly in the phosphate side, the pH 9.0 caused bigger mineral precipitation as an basic layer with homogeneous microstructure, while the pH 7.0 induced additional specific and elaborated crystals under '*hexagonal*' or '*cuttlebone*' shapes, when the membrane is immersed in HCl/succinic or citric acids, respectively.

Proteins, Lipids and Gags Analyses

The mean protein, lipid and GAG contents (Table 1) showed a clear tendency to decrease, between time 0 and 6 h after bathing, being significant($p < 0.05$) in the experiments at pH 9.0 (with NaOH) where the mineral precipitation was also more intense. In this condition, while protein and lipid contents decreased significantly around 50 %, the GAG had a much smaller decrease. Additionally, at pH 6.0 and 7.0, the GAG contents had a strong increase on the final solutions.

Scanning Observations

With the present SEM observations, it was shown that the solutions bathing cellulose membranes at pH 7.0

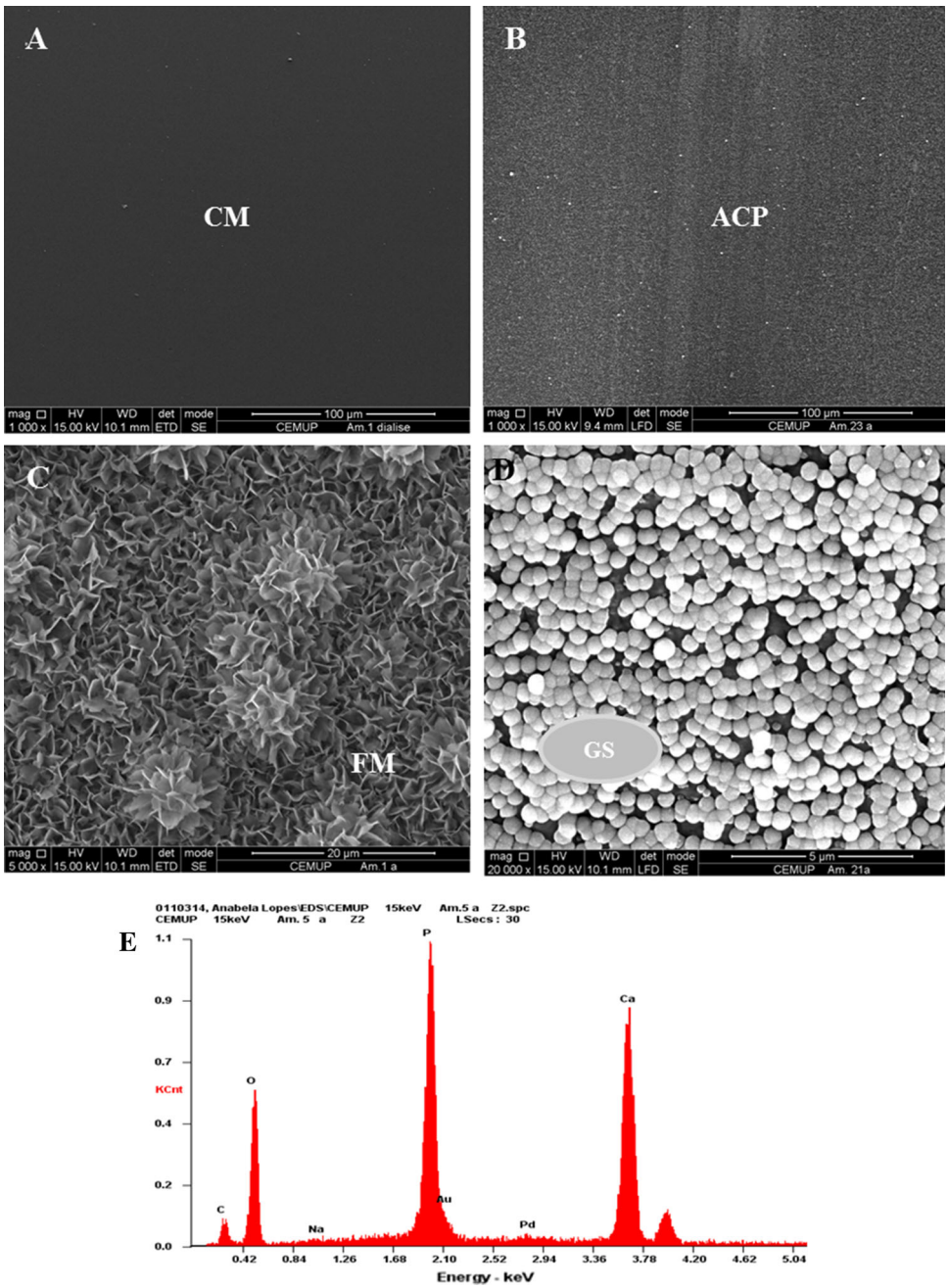

Fig. 1 SEM images of phosphate side of the cellulose membrane at different pHs. **a** Only the cellulose membrane (CM) surface without any mineral deposit at pH 6.0. **b** With a smooth mineral layer of amorphous calcium phosphate base (ACP) at pH 7.0. **c** A magnification of the same amorphous mineral layer under succinic solution at pH7 presenting a peculiar shape as a foliate microstructure (FM). **d** Observing a clear and well spread granular structure (GS) at pH 9.0. **e** Amorphous mineral layer EDS

and 9.0 are more efficient than at pH 6.0 concerning the amount of calcium phosphate deposits as a homogeneous base (primary phase) and the specificity on the crystalline microstructure (second phase) formed over the mineral base mainly at pH 7.0 (Figs. 1, 2, 3, 4).

pH 6.0

None of the experiments carried out at a pH 6.0 (with HCl, citric, succinic acids) with/without organic fluids of *A. cygnea* could induce any kind of mineral precipitation in both surfaces of the cellulose membrane (Fig. 1a). Instead, these membranes were more fragile and flexible after 6 h of bathing, probably due to interface degradation of the cellulose membranes in what concern the structure dynamic and electric-physical properties.

pH 7.0

The actual experiments carried out at a pH 7.0 (with HCl, succinic and citric acids) represented the most efficient

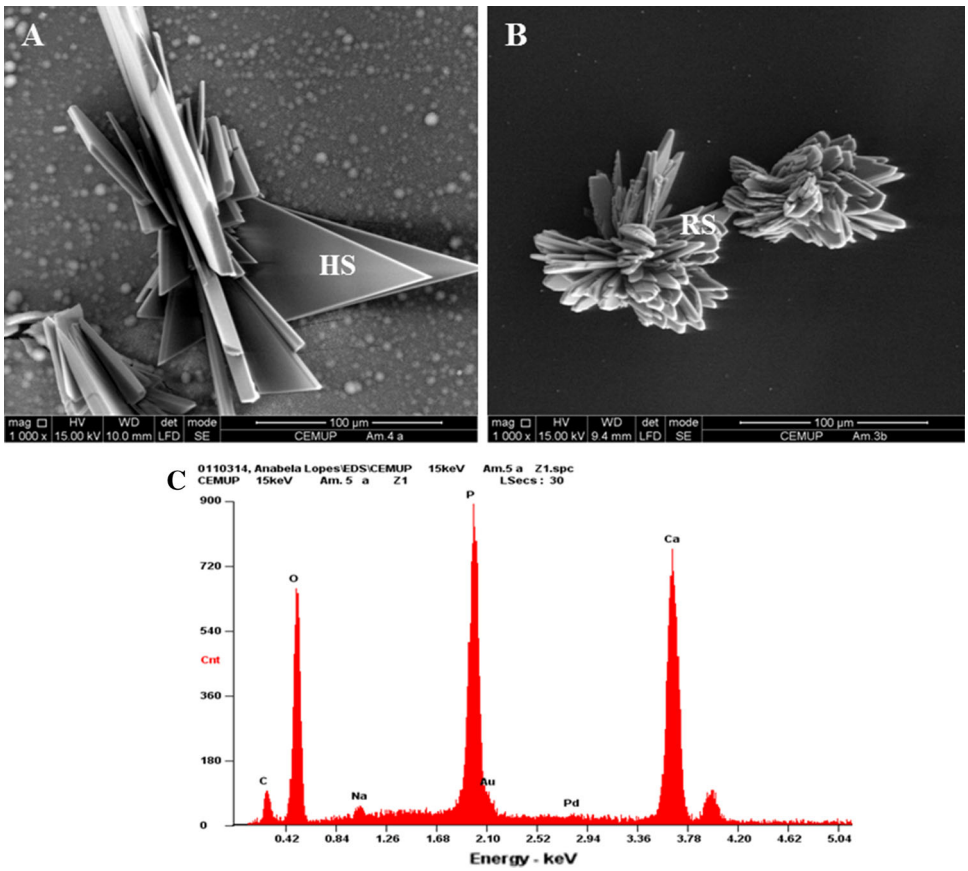

Fig. 2 SEM images of the cellulose membrane bathed in succinic acid solutions mixed with biological fluids of *A. cygnea* at pH 7.0. **a** Large clusters of crystalline formations composed by calcium phosphate under hexagonal shapes (HS) on the phosphate side. **b** Observing clusters of rosaceous structures (RS) composed by calcium phosphate crystals under hexagonal forms on the calcium side. **c** Crystal EDS

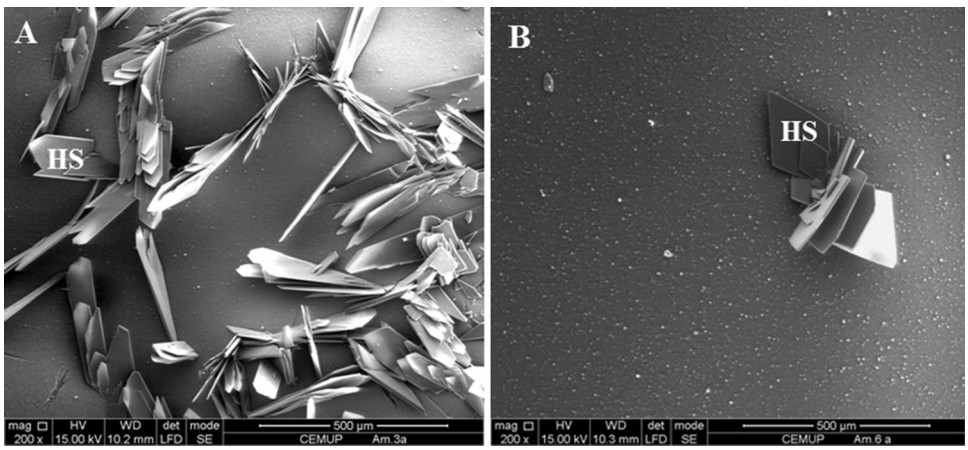

Fig. 3 SEM images of the cellulose membrane bathed in HCL solutions mixed with biological fluids of *A. cygnea* at pH 7.0. **a** Showing several clusters of crystalline formations composed by calcium phosphate under *hexagonal shapes* (HS) on phosphate side. **b** Observing a single cluster of HS on the calcium side

conditions for mineralization events on cellulose membranes since many crystalline microstructures were produced with specific shapes, over the homogeneous layer (Figs. 2, 3, 4). So, only with HCl or succinic acid solutions, laminar crystalline formations of calcium phosphate under hexagonal shape (some on clusters) were observed in both sides of the membrane, but mainly in the phosphate side (Figs. 2 and 3). The preferential ionic calcium movement towards the phosphate chamber conditioned all of the subsequent mineralization processes in cellulose membranes.

pH 9.0

All assays carried out with synthetic solutions at pH 9.0 (with NaOH) isolated or mixed with biological fluids of *A. cygnea* induced an intense precipitation of calcium phosphate, apparently without any crystalline microstructure. However, when the biological fluids were included in the solutions, this homogeneous layer, when observed with SEM at higher magnification (Fig, 1d), showed typical '*globular*' micro-concretions of calcium phosphate, mainly in the phosphate surface.

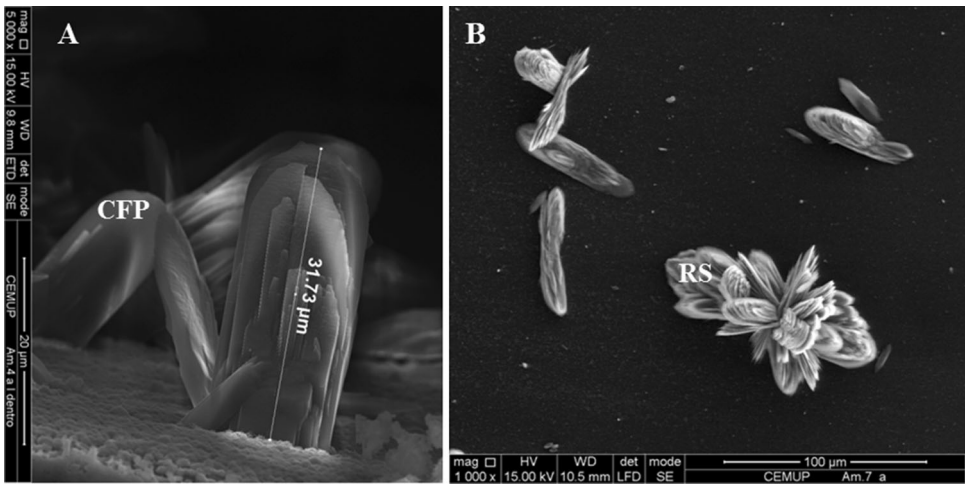

Fig. 4 SEM images at phosphate side of the cellulose membrane at pH 7.0. **a** Observing crystalline formations of calcium phosphate under cuttlebone shapes (CFP), when bathing in citric acid synthetic solutions. **b** Exhibiting clusters of rosaceous structures (RS) composed by calcium phosphate crystals under cuttlebone forms, when bathing in citric synthetic solutions mixed with biological fluids of *A. cygnea*

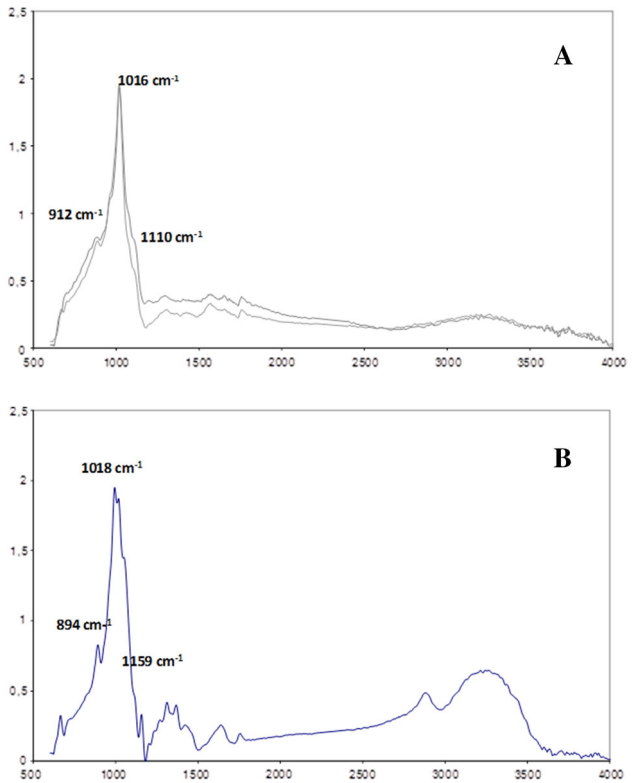

Fig. 5 FTIR spectra of cellulose membrane accomplished in a total of 18 samples on the mineralized phosphate chamber side, 6.0 h after in different bathing solutions with or without organic fluids from *A. cygnea* **a** showing the curves average of attenuated transmission reflectance from samples S1, S2, C1 and H samples at pH 7.0; **b** with S2, C2 and N curves average exhibiting the attenuated transmission reflectance from membrane samples

Nature of Crystal Phase

FTIR Analyses

ATR-IR spectra observed in Fig. 5a, b, shown that calcium precipitates mainly in the phosphate side, being characterized by a strong ν_3 asymmetrical vibration at 1016 cm^{-1} (samples with succinic acid at pH7 (S1), succinic acid with haemolymph at pH7 (S2), citric acid at pH7 (C1) and HCl at pH7 (H)—Fig 5a), corresponding to tetrahedral molecule of PO_4^{3-}. The non-protonated PO_4^{3-} anion has tetrahedral symmetry and belongs to the point group Td with one active v_3 band centred at 1011 cm^{-1}, whereas the ν_1 vibration is inactive. The v_3 band centred at 1016 cm^{-1} is degenerated at about 1100 and 912 cm^{-1}, where both bands occur as shoulders at fundamental vibration due to distorted tetrahedral molecule. Fundamental vibrational frequency (v_3) is correlated with both vibration planes at 1010 and 1070 cm^{-1} that correspond to HPO_4^{2-} anion. The fundamental P-O stretching band is very sharp in the analyzed samples (S1, S2, C1, H), which suggests a good crystallization, low symmetry with a disordered structure of the material analyzed. Few samples exhibit the v_1 band well active at 880 cm^{-1}, so that a total of four bands are present for this phosphate species (Fig. 5a).

Samples S2, S3 (with succinic acid and extrapallial fluid at pH7), C2 (with citric acid and haemolymph at pH7) and N (pH 9 with haemolymph) show a large $v_3$band centred at 1016 cm^{-1} and a vibrational plane at about 894 and 1159 cm^{-1} (Fig. 5b), beside the typical ν_3 fundamental vibration previously described. Band at 894 cm^{-1} corresponds to P–O–P stretching band. So, based on the FTIR data, it is possible to conclude that the calcium phosphate layer precipitated during the 6.0 h period under a preliminary hydroxyapatite mineral phase.

X-Ray Analyses

In general, the X-ray analyses of calcium precipitates, mainly in the phosphate side, confirmed the presence of a preliminary microstructure with a weak crystallization

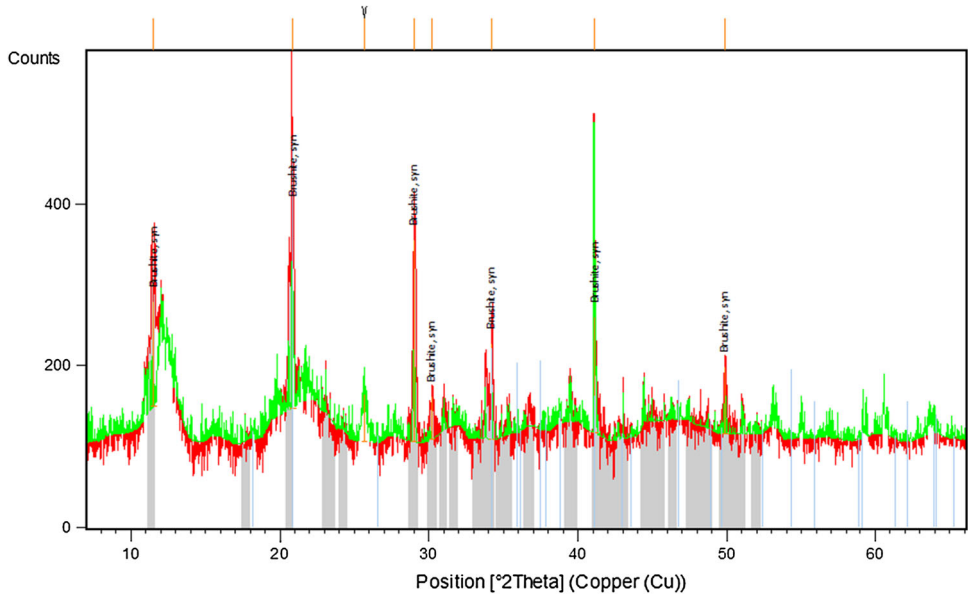

Fig. 6 The X-ray analyses showed a not well elaborated crystal structure, which can be interpreted as a precursor of the apatite structure under the brushite crystal phase with the $CaPO_3(OH)\cdot 2H_2O$

Table 1 Variations after 6.0 h of organic molecules contents in calcium side on the HCl, succinic and citric acid solutions at pH 6.0 and 7.0 ($n = 54$) and on the NaOH solution at 9.0 ($n = 18$), all mixed with haemolymph or extrapallial fluids bathing the cellulose membranes

	Haemolymph		Extrapallial	
	$t = 0$ h	$t = 6$ h	$t = 0$ h	$t = 6$ h
Total proteins (mg/ml)				
pH6	840.83 ± 24.41	352.35 ± 68.92*	825.00 ± 22.41	366.96 ± 63.71*
pH7	985.14 ± 16.94	483.99 ± 92.09*	939.31 ± 26.98	454.42 ± 94.80*
pH9	989.31 ± 29.21	205.63 ± 45.62*	916.11 ± 25.17	276.51 ± 43.49*
Total lipids (mg/dl)				
pH6	108.73 ± 10.87	29.84 ± 14.10*	72.89 ± 3.49	29.58 ± 14.66*
pH7	106.59 ± 10.59	33.24 ± 19.14*	65.92 ± 1.96	23.32 ± 8.12*
pH9	102.06 ± 9.23	16.51 ± 3.45*	51.62 ± 9.31	19.23 ± 3.87*
Total GAGs (mg/ml)				
pH6	73.27 ± 7.87	100.48 ± 26.72*	48.69 ± 3.30	103.25 ± 25.05*
pH7	60.46 ± 4.59	105.72 ± 29.92*	81.80 ± 6.34	116.69 ± 23.42*
pH9	49.64 ± 8.56	46.00 ± 7.84	81.27 ± 6.71	67.08 ± 15.58*

* Represents significant differences ($p < 0.05$) relative to the control

phase, which can be interpreted as an apatite precursor under a brushite crystal system (Fig. 6). It is generally accepted that brushite is formed by interaction or reaction between calcium and phosphate solutions under a primitive crystal structure.

Integrative observation of results

In the present research, it was possible to observe that specific organic acids such as the succinic and citric or even the HCl, with or without bivalve fluids, can regulate typical structures in the calcium phosphate precipitates. The actual results showed a homogeneous calcium phosphate deposit, mainly at phosphate side, as a structural base covering the cellulose membrane in most experimental situations, except at pH 6.0. This layer increased in thickness, mainly with the alkaline media solution at pH 9.0. Alternatively, it may be covered by hexagonal-shaped crystals occurring predominantly in the phosphate chamber, at pH 7.0 with HCl titration. With the citric or succinic solutions at same pH 7.0, the crystalline microstructures exhibited distinct shapes, particularly *cuttlebone* or thicker hexagonal shapes, also predominant in the phosphate side. When solutions are mixed with the organic fluid of *A. cygnea,* these crystal forms increased under agglomerated and rosaceous structures. Although proteins, lipids and GAGs are inductors of vaterite/aragonite/calcite crystals in the natural bivalve shell formation, a brushite crystal polymorphism as a preliminary apatite phase was detected in the present study, under semi-artificial conditions.

Discussion

Regenerated cellulose membranes have appropriate structure for medical applications, since they have selective behaviour allowing the permeation of small ions/molecules but reject the transport of proteins or macromolecules (Sakai 1994). In order to establish a relevant line of thought about the present results using commercial cellulose membranes comparatively to the previous study with chitosan membranes (Lopes et al. 2010), it is convenient to emphasize some clear differences about the physical properties of both membranes. In general, the chitosan membrane induced selective movements of ions and particles influenced by the positively charged pores (cationic polyelectrolyted due to the presence of amine groups –NH2), explained by the electrostatic attraction or repulsion between the solute and the membrane, on the contrary the cellulose membranes exhibited a relevant selective permeability and electrical resistance based on the slight negative charges due to the oxidation of –CH2OH groups to –COOH (Reid and Breton 1959; Strathmann 1981; Seo et al. 1991; Matsuyama et al. 1998; Ehrlich et al. 2006; Lopes et al. 2010; Irvine et al. 2013). This could play a notable role when the transport of electrolyte solutions or charged particles is considered (Kimura et al. 1984; 1986, Vázquez et al. 2008; Romero et al. 2013). According to Asaka (1990) and Romero et al. (2012, 2013), solutes diffusion depend on the electrical parameters such as the effective fixed charge and ions transport numbers, as well as on diffusion coefficients related with friction interactions and, consequently, with pore size. So, the net rate of a given solute transfer (at a certain temperature, viscosity and mixing rate) across such semi-permeable membrane will increase with greater electrochemical gradients between the two solutions and, inversely, will decrease with the greater size and shape of solutes or molecules.

The present results show that cellulose membranes exhibit very distinct physical-chemical properties (electrochemical field, ionic pore diffusion, mineral precipitation interface and film biomechanical adhesive role) when compared to those using chitosan membranes (Lopes et al. 2010).While the negative phosphate ions diffuse, intensely attracted by positive pores, towards the calcium chamber across the chitosan membranes; the calcium ions preferentially move to the opposite phosphate chamber using cellulose membranes, due to the slight negative pores with subsequent cation affinity and to an eventual and gradual reduction of the pore size. According to Reid and Breton (1959), the presence of hydrogen bonding (from the water bathing) to carboxyl groups in the cellulose membrane would gradually make the film act as a cation exchanger with a consequent high resistance to anions. Then, as smaller size and positive charge is the ion, more it should promote stronger diffusion. This also explains the higher calcium diffusion than the phosphate ion, across the membrane. Since the results show distinct ionic diffusion mechanisms in both membranes, this specificity can subsequently induce different biomineralization kinetics when biological fluid molecules were added. In fact, an intense formation of typical minerals combined with organic molecules is observed exclusively in the calcium side of chitosan assays, while the contrary occurs in cellulose membranes where specific crystals can also develop, but mainly in phosphate side. These opposite patterns may be supported by the additional diffusion of smaller positive organic molecules (as negative charged amino-acids or peptides) from the calcium towards the phosphate chamber only in the cellulose membrane, possibly also due to a higher molecular weight cutoff. This suggests that the different diffusion kinetics will determine a primary phase of calcium phosphate, as a brushite, in the cellulose membrane, while it is more elaborate form, as a hydroxyapatite, in chitosan membrane (Lopes et al. 2010) where the phosphate ion is the major diffuser. Moreover, in the last condition, the whole organic molecules (haemolymph or extrapallial fluids) are mostly kept in the calcium side promoting a higher and complete biomineralization mechanism, as a mimetic system of the shell matrix. Furthermore, regarding the calcium and phosphate content evaluations, in all sets with the cellulose membrane, they revealed a significant difference on the positive ions as calcium and small molecules, mostly directed towards the phosphate chamber. In opposition to this mechanism, in chitosan membrane assays, it was showed the phosphate almost exclusively moving towards the calcium chamber. This difference is mainly supported by the presence of amine groups $–NH_2$ in the chitosan membrane while by the groups to –COOH in the cellulose membrane. On the other hand, relatively to the mineralization phenomena, the rate of Ca^{2+} and PO_4^{3-} ions deposition from solution surely depended on the surface functional groups. That is, the functional groups influence the barrier to nucleation and thus the ability to form critical size nuclei (Toworfe et al. 2006). This behaviour is attributed to surface charges which determine the solid/cluster interfacial energies involved in the nucleation of Ca–P particles from Ca^{2+} and $PO4^{3-}$ species in super-saturation (Yang et al. 1999). Thus, this may suggest that the amine terminated surface as in the chitosan membrane adsorbs more PO_4^{3-}; to the contrary, the abundant –OH or –COOH groups on the cellulose surface will contribute more to the Ca^{2+} bioactivity (Tanahashi and Matsuda 1997; Toworfe et al. 2006).

Generally, minerals are produced synthetically in non-biological processes, where the degree of control over nucleation and growth can be achieved by a deterministic

process from a modifier organic matrix. The perception of the physical principles of crystallization from solutions is fundamental to understand the biomineralization mechanisms. On the other hand, the presence of organic matrixes can induce specific epitaxial phenomena when in the contact with ionic solutions promoting very typical and exuberant crystalline microstructures. Since this experimental methodology was based mainly on the combination of biosynthetic membranes and organic fluids of *A. cygnea* (not usual), we try to emphasize particularly some differences between cellulose and chitosan membranes behaviour (Lopes et al. 2010) under similar conditions and parameters.

In this context, the present results concerning the protein, lipid and GAG contents using cellulose membrane, opposite results were obtained with the reduced GAGs contents when using chitosan membranes, mainly at pH 6.0, and 7.0 (Lopes et al. 2010). On the other hand, the present cellulose results on proteins and lipids contents exhibited a similar (although stronger) decreasing tendency, when compared with the chitosan membrane studies. In general, proteins, lipids and GAGs are referred as shell biomineralizing molecules, being GAGs in particular, most appropriate candidates for the nucleation process in the shell nacreous layer of *A. cygnea* (Moura et al. 2003b; Lopes-Lima et al. 2005). Thus, based on these principles, concerning the proteins and lipids compounds, the results in cellulose assays showed an expected variation, as found in chitosan membrane. On the contrary, an unexpected increasing tendency on GAGs contents in the actual experiments seems to reflect an inversed behaviour. We can speculate that these large molecules were strongly forced to diffuse by a gradient process, from the calcium to the phosphate side, which possibly caused GAGs cleavage into smaller particles due to eventual friction through the pores. This aggressive mechanism possibly caused an exposition of more staining reactive terminal in GAGs, leading to higher measurement levels in the cellulose data. This explanation is also supported by the occurrence of GAG content decrease in the calcium chamber of chitosan membranes, and in simultaneous, by lack of calcium deposition in phosphate chamber (due to a total absence of GAGs and other small molecules diffusion across the chitosan membrane). Yet, the detectable reduction tendency in the cellulose membrane of GAGs content at pH 9.0 may be well correlated with a visible involvement on the stronger mineral deposition which annulated any measurement artefact (contrary to the pH 6.0 and 7.0 situations).

These assays generally suggest a clear specific physical role of the organic molecules in the chitosan membranes, being more active in the calcium chamber at acid pH (inserted fluid side), while in the cellulose membrane there were more interactive in the phosphate chamber (without fluid side) at more alkaline pHs. This suggests that in cellulose at alkaline pH, the membrane becomes more negative attracting greater calcium ion flux towards the phosphate chamber, on contrary, the chitosan membrane at acid pH is induced for a more positive interface potentiating higher phosphate ion flux into the calcium chamber. This thinking about pH effect is possible, if combined with the pore size property which seems greater in the chitosan case allowing easily phosphate diffusion, while it is smaller in the cellulose membrane facilitating only calcium (or smaller molecules) diffusion. In addition, the absence of any detectable organic molecules content, in the phosphate chamber of cellulose membrane, associated to the precipitation of specific calcium phosphate form, may indicate that, at least, the smaller positive molecules had probably an effective (but silent) biomineral intervention. This agrees with Mohamed et al. (1995); Matsuyama et al. (1998); Childress and Elimelech (1996); Cui et al. (2008) and Radhakrishnan et al. (2010), stating that in acidic solution, amine groups of chitosan membrane are protonated to $-NH_3^+$ becoming more positive charged and so attracting more phosphate ion diffusion, while in alkaline solution, the cellulose membrane becomes enriched with –OH or –COOH groups and thus attracting more calcium ion diffusion. As a conclusion, the effectiveness of the charged groups in the membranes is explained by the counter-ion binding mechanism (Ilani 1970; Kimura et al. 1984; Childress and Elimelech 1996). At summary, the membranes possess pH-sensitive dissociable functional group and separates molecules by both size exclusion and electrostatic effects (Manttari et al. 2006; Luo et al. 2012; Luo and Wan 2013).

Relative to the scanning observations, the cellulose experiments revealed an opposite pattern to the chitosan membranes (Lopes et al. 2010) where at the same pH (6.0) was mostly efficient producing crystalline microstructures than at pH 7.0 and 9.0. Additionally, there were significantly less deposits formed in the calcium chamber in cellulose experiments, while a very intense mineral precipitation was here exclusively observed using chitosan membranes, due to the fact that the biomineral formation occurred better in the biological fluid side (inserted in the calcium chamber). Under pH 6.0 condition, no mineral precipitation was stated in cellulose membrane but, in contrast, the chitosan membrane (Lopes et al. 2010) revealed excellent and more effective calcium phosphate mineral adsorption in the calcium side with specific hexagonal and *rosaceous* shapes, mainly with HCl and succinic solution, respectively. This difference suggests a very specific mechanical and electrochemical behaviour at this pH depending on the matrix composition and structural organization of both membranes, as we already justified. In synthetic solutions, at pH 7.0, conditions are mixed with haemolymph and extrapallial fluids, the cellulose membrane showed crystalline formations, similar in all assays,

specifically under '*rosaceous*' structures, with a higher tendency for cluster formation mainly in the phosphate side. In addition, using only synthetic citric acid solution peculiar calcium phosphate formations, with very typical '*cuttlebone*' shape, were observed (some also on clusters) in both sides of the membrane, still predominant in the phosphate side. Differently, chitosan experiments under the same conditions showed an amorphous calcium deposition, and only in the calcium chamber at general pH 7.0, with an aggravating fact that, under the control and citric acid, no mineralization process was found (Lopes et al. 2010). Attending the pH 9.0 assays in the cellulose experiments, the mineral microspherules structures were present while in the chitosan were absent (Lopes et al. 2010). However, under SEM observation, the deposition of a homogeneous microstructure as a primary calcium phosphate layer, with or without any specific mineral microspherules, occurred in both cellulose and chitosan membrane at this pH, respectively. Once again, mechanical and electrochemical behaviour at pH 9.0 and 7.0 depend probably on the matrix composition, structural and electrochemical organization of both membranes.

The FTIR and X-ray techniques analyzed distinct physical behaviour between both cellulose and chitosan membranes with clear differences on the biomineralization process submitted to the similar conditions. In fact, while for the cellulose membrane the analyses showed a very primitive crystallization phase, as a brushite crystal in the phosphate side, for the chitosan membrane (Lopes et al. 2010), a more defined and elaborated crystal microstructure, as a primary hydroxyapatite phase, was observed mainly in the calcium side. Different authors (Chang et al. 2003; Ferreira et al. 2003; Anee et al. 2004; Resende et al. 2006; Štulajterová and Medvecký 2008) suggested that brushite could also be formed by chemical reaction between a phosphate solution and bicarbonate-H_2O solution when combine with calcium, which is according the media composition in the present assays.

Conclusion

The facts showed that the deterministic influence of the organic matrix from the organic fluids of *A. cygnea,* may change according to the specificity of the microhabitat, depending on the artificial medium composition and biosynthetic membranes. While the fluids promote aragonite crystals in the inner nacreous shell, it may also induce apatite-brushite or hydroxyapatite under specific conditions in synthetic cellulose or chitosan membrane, respectively, if in the presence of phosphates. The cellulose membranes evidenced high specificity relative to the diffusion mechanisms of calcium and phosphate ions and smaller organic molecules. This phenomenon is mainly due to a particular physical and mechanical structure, such as pore size (MWCO), slightly negative charges by the presence of hydroxyls or carboxyls groups, as well as the pH regulation effect on the interface of liquid-membrane. At the end, these experiments seem to show some interesting properties of chitosan and cellulose membrane which approaches partially to the biological epithelia by their diversity on the ion and molecules diffusion supported on the specificity of electrochemical gradient and of membranes structure associated to the electric field. Obviously, the present study indicates a useful and versatile tool in order to adapt easily and efficiently to the biomedical or technological applications.

Acknowledgments The authors were supported by Fundação para a Ciência e Tecnologia (FCT) under projects PTDC/MAR/098066/2008, PTDC/AAC-AMB/117688/2010; COST Action TD0903.

References

Addadi L, Weiner S (1992) Control and design principles in biological mineralization. Angew Chem Int Ed 31:153–169. doi:10.1002/anie.199201531

Albrecht W, Santoso F, Lutzow K, Weigel T, Schomacker R, Lendlein A (2007) Preparation of aminated microfiltration membranes by degradable functionalization using plain PEI membranes with various morphologies. J Membr Sci 292:145–157. doi:10.1016/j.memsci.2007.01.027

Anee TK, Palanichamy M, Ashok M, Sundaram NM, Kalkura SN (2004) Influence of iron and temperature on the crystallization of calcium phosphates at the physiological pH. Mater Lett 58:478–482. doi:10.1016/S0167-577X(03)00529-9

Avramescu ME, Sager WFC, Mulder MHV, Wessling M (2002) Preparation of ethylene vinylalcohol copolymer membranes suitable for ligand coupling in affinity separation. J Membr Sci 210:155–173. doi:10.1016/S0376-7388(02)00409-X

Belcher AM, Wu XH, Christensen RJ, Hansma PK, Stucky GD, Morse DE (1996) Control of crystal phase switching and orientation by soluble mollusc-shell proteins. Nature 381:56–58. doi:10.1038/381056a0

Büyüktuncel E, Bektas S, Genc Ö, Denizli A (2001) Poly(vinylalcohol) coated/Cibacron Blue F3GA-attached polypropylene hollow fiber membranes for removal of cadmium ions from aquatic systems. React Funct Polym 47:1–10. doi:10.1016/S1381-5148(00)00054-7

Carter JG (1990) Evolutionary significance of shell microstructure in the Palaeotaxodonta, Pteriomorphia and Isofilibranchia (Bivalvia: Mollusca). In: Carter JG (ed) Skeletal biomineralization: patterns, processes and evolutionary trends, vol 1. Van Nostrand Reinhold, New York, pp 35–296

Chang MC, Ko CC, Douglas WH (2003) Preparation of hydroxyapatite-gelatin nanocomposite. Biomaterials 24:2853–2862. doi:10.1016/S0142-9612(03)00115-7

Checa AG, Jiménez-López C, Rodríguez-Navarro A, Machado JP (2006) Precipitation of aragonite by calcitic bivalves in Mg-enriched marine waters. Mar Biol 150:819–827. doi:10.1007/s00227-006-0411-4

Chen ZA, Deng MC, Yong C, He GH, Ming W, Wang JD (2004) Preparation and performance of cellulose acetate/polyethyleneimine blend microfiltration membranes and their applications. J Membr Sci 235:73–86. doi:10.1016/j.memsci.2004.01.024

Childress AE, Elimelech M (1996) Effect of solution chemistry on the surface charge of polymeric reverse osmosis and nanofiltration membranes. J Membr Sci 119:253–268. doi:10.1016/0376-7388(96)00127-5

Colton CK, Smith KA, Merrill EW, Farrell PC (1971) Permeability studies with cellulosic membranes. J Biomed Mater Res Part B 5:459–488. doi:10.1002/jbm.820050504

Cui Z, Xiang Y, Si J, Yang M, Zhang Q, Zhang T (2008) Ionic interactions between sulfuric acid and chitosan membranes. Carbohyd Polym 73:111–116

Darder M, Aranda P, Hernández-Vélez M, Manova E, Ruiz-Hitzky E (2006) Encapsulation of enzymes in alumina membranes of controlled pore size. Thin Solid Films 495:321–326

De Yoreo J, Vekilov P (2003) Principles of crystal nucleation and growth. In: Biomineralization. Dove PM, De Yoreo J, Weiner S (eds) Reviews in Mineralogy and Geochemistry, 54:57–94. doi:10.2113/0540057

Ehrlich H, Krajewska B, Hanke T, Born R, Heinemann S, Knieb C, Worch H (2006) Chitosan membrane as a template for hydroxyapatite crystal growth in a model dual membrane diffusion system. J Membr Sci 273:124–128

Falini G, Albeck S, Weiner S, Addadi L (1995) Control of aragonite or calcite polymorphism by mollusk shell macromolecules. Science 271:67–69. doi:10.1126/science.271.5245.67

Farrell PC, Babb AL (1973) Estimation of the permeability of cellulosic membranes from solute dimensions and diffusivities. J Biomed Mater Res 7:275–300

Ferreira A, Oliveira C, Rocha F (2003) The different phases in the precipitation of dicalcium phosphate dehydrate. J Cryst Growth 252:599–611. doi:10.1016/S0022-0248(03)00899-6

Han W, Liu CX, Bai RB (2007) A novel method to prepare high chitosan content blend hollow fiber membranes using a non-acidic dope solvent for highly enhanced adsorptive performance. J Membr Sci 302:150–159. doi:10.1016/j.memsci.2007.06.039

Ilani A (1970) Discrimination between monovalent and divalent cations by hydrophobic solvent-saturated membranes containing fixed negative charges. J Membr Biol 3:223–240

Irvine GJ, Rajesh S, Georgiadis M, Phillip WA (2013) Ion selective permeation through cellulose acetate membranes in forward osmosis. Environ Sci Technol 47:13745–13753

Janis CM (1995) Correlations between craniodental morphology and feeding behavior in ungulates: reciprocal illumination between living and fossil taxa. In: Thomason JJ (ed) Functional morphology in vertebrate paleontology. Cambridge University Press, Cambridge, pp 76–98

Javaux EJ, Knoll AH, Walter MR (2001) Morphological and ecological complexity in early eukaryotic ecosystems. Nature 412:66–69. doi:10.1038/35083562

Karppi J, Akerman S, Akerman K, Sundell A, Penttila I (2010) Adsorption of metal cations from aqueous solutions onto the pH responsive poly(vinylidene fluoride grafted poly(acrylic acid) (PVDF–PAA) membrane. J Polym Res 17:71–76. doi:10.1007/s10965-009-9291-x

Kimura Y, Lim HJ, Iijima T (1984) Membrane potentials of charged cellulosic membranes. J Membr Sci 18:285–296

Kimura Y, Lim HJ, Iijima T (1986) Permeability of alkali chlorides through charged cellulosic membranes. Angew Makromol Chemie 138:151–158

Koyuncu I, Arikan OA, Wiesner MR, Rice C (2008) Removal of hormones and antibiotics by nanofiltration membranes. J Membr Sci 309:94–101. doi:10.1016/j.memsci.2007.10.010

Kroger N, Deutzmann R, Bergsdorf C, Sumper M (2000) Species-specific polyamines from diatoms control silica morphology. Proc Nat Acad Sci USA 97:14133–14138. doi:10.1073/pnas.260496497

Lay WCL, Liu Y, Fane AG (2010) Impacts of salinity on the performance of high retention membrane bioreactors for water reclamation: a review. Water Res 44:21–40. doi:10.1016/j.watres.2009.09.026

Leoni L, Boiarski A, Desai TA (2002) Characterization of nanoporous membranes for immunoisolation: diffusion properties and tissue effects. Biomed Microdev 4(2):131–139

Liu CX, Bai RB (2005) Preparation of chitosan/cellulose acetate blend hollow fibers for adsorptive performance. J Membr Sci 267:68–77. doi:10.1016/j.memsci.2005.06.001

Liu CX, Bai RB (2006) Preparing highly porous chitosan/cellulose acetate blend hollow fibers as adsorptive membranes: effect of polymer concentrations and coagulant compositions. J Membr Sci 279:336–346. doi:10.1016/j.memsci.2005.12.019

Lopes A, Lopes-Lima M, Bobos I, Ferreira J, Gomes S, Reis R, Mano J, Machado J (2010) The effects of *Anodonta cygnea* biological fluids on biomineralization of chitosan membranes. J Membr Sci 364:82–89

Lopes-Lima M, Ribeiro IRA, Pinto RA, Machado J (2005) Isolation, purification and characterization of glycosaminoglycans in the fluids *of Anodonta cygnea*. Comp Biochem Physiol A 141:319–326. doi:10.1016/j.cbpb.2005.06.007

Lopes-Lima M, Rocha A, Gonçalves F, Andrade J, Machado J (2010) Microstructural characterization of inner shell layers in the freshwater bivalve *Anodonta cygnea*. J Shellfish Res 29:969–973. doi:10.2983/035.029.0431

Lopez E, Vidal B, Berland S, Camprasse S, Camprasse G, Silve C (1992) Demonstration of the capacity of nacre to induce bone formation by human osteoblasts in vitro. Tissue Cell 24:667–679. doi:10.1016/0040-8166(92)90037-8

Luo J, Wan Y (2013) Effects of pH and salt on nanofiltration—a critical review. J Membr Sci 438:18–28

Luo J, Cao W, Ding L, Zhu Z, Wan Y, Jaffrin MY (2012) Treatment of dairy effluent by shear-enhanced membrane filtration: the role of foulants. Sep Purif Technol 96:194–203

Mahendran R, Malaisamy R, Mohan DR (2004) Cellulose acetate and polyethersulfone blend ultrafiltration membranes. Part I: Preparation and characterizations. Polym Adv Technol 15:149–157

Mano JF (2008) Viscoelastic properties of chitosan with different hydration degrees as studied by dynamic mechanical analysis. Macromol Biosci 8:69–76. doi:10.1002/mabi.200700139

Mano JF, Silva GA, Azevedo HS, Malafaya PB, Sousa RA, Silva SS, Boesel LF, Oliveira JM, Santos TC, Marques AP, Neves NM, Reis RL (2007) Natural origin biodegradable systems in tissue engineering and regenerative medicine: present status and some moving trends. J R Soc Interf 4:999–1030. doi:10.1098/rsif.2007.0220

Manttari M, Pihlajamaki A, Nystrom M (2006) Effect of pH on hydrophilicity and charge and their effect on the filtration efficiency of NF membranes at different pH. J Membr Sci 280:311–320

Matsuyama H, Kitamura Y, Naramura Y (1998) Diffusive permeability of ionic solutes in charged chitosan membrane. J Appl Polym Sci 72(3):397–404

Mehta A, Zydney AL (2005) Permeability and selectivity analysis for ultrafiltration membranes. J Membr Sci 249:245–249

Mohamed NS, Subban RH, Arof AK (1995) Polymer batteries fabricated from lithium complexed acetylated chitosan. J Power Sour 56:153–156

Mount AS, Wheeler P, Paradkar RP, Snider D (2004) Hemocyte-mediated shell mineralization in the eastern oyster. Science 304:297–300. doi:10.1126/science.1090506

Moura G, Guedes R, Machado J (1999) The extracellular mineral concretions in *Anodonta cygnea* (L.): different types and manganese exposure-caused changes. J Shellfish Res 18:645–650

Moura G, Vilarinho L, Santos AC, Machado J (2000) Organic compounds in the extrapallial fuid and haemolymph of *Anodonta cygnea* (L.) with emphasis on the seasonal biomineralization process. Comp Biochem Physiol B 125:293–306. doi:10.1016/S0305-0491(99)00192-3

Moura G, Guedes R, Machado J (2001) Annual compositional and morphological variations in the nacreous layers of the shell of *Anodonta cygnea*. Malacol Rev 33–34:106–111

Moura G, Machado J, Coimbra J (2003a) Insights on nacre formation in the freshwater clam, *Anodonta cygnea* (L.): an overview. In: Kobayashi I, Ozawa H (eds) Biomineralization (BIOM2001): formation, diversity, evolution and application, proceedings of the 8th international symposium on biomineralizations. Tokai University Press, Kanagawa, pp 129–132

Moura G, Almeida MJ, Machado MJ, Vilarinho L, Machado J (2003b) The action of environmental acidosis on the calcification process of *Anodonta cygnea* (L.). In: Kobayashi I, Ozawa H (eds) Biomineralization (BIOM2001): formation, diversity, evolution and application, proceedings of the 8th international symposium on biomineralizations. Tokai University Press, Kanagawa, pp 178–182

Nielsch K, Choi J, Schwirn K, Wherpohn RB, Gösele U (2002) Self-ordering regimes of porous alumina: the 10 % porosity-rule. Nano Lett 2:677–680

Nunes SP, Peinemann KV (2006) Membrane technology in the chemical industry. John-Wiley and Sons, Weinheim

Ohata R, Tomita N, Ikada Y (2004) Effect of a static magnetic field on ion transport in a cellulose membrane. J Colloid Interf Sci 270:413–416. doi:10.1016/j.jcis.2003.09.035

Pappenheimer JR (1953) Passage of molecules through capillary walls. Physiol Rev 33(3):387–423

Radhakrishnan R, Begum A, Sri S (2010) Protonation of the NH_2 groups through crosslinking chitosan membranes with H_2SO_4. Int J Curr Res 11:085–088

Reid CE, Breton EJ (1959) Water and ion flow across cellulosic membranes. J Appl Polym Sci 1:133–143. doi:10.1002/app.1959.070010202

Ren J, Li Z, Wong F (2006) A new method for the prediction of pore size distribution and MWCO of ultrafiltration membranes. J Membr Sci 279:558–569

Renkin EM (1954) Filtration, diffusion and molecular sieving through porous cellulose membranes. Gen Physiol 38(2):225–243

Resende NS, Nele M, Salim VMM (2006) Effects of anion substitution on the acid properties of hydroxyapatite. Thermochim Acta 451:16–21

Romero V, Vega V, García J, Prida VM, Hernando B, Benavente J (2012) Ionic transport across tailored nanoporous anodic alumina membranes. J Colloid Interf Sci 376:40–46

Romero V, Vázquez MI, Benavente J (2013) Study of ionic and diffusive transport through a regenerated cellulose nanoporous membrane. J Membr Sci 433:152–159

Sakai K (1994) Determination of pore size and pore size distribution: 2 dialysis membranes. J Membr Sci 96:91–130

Santos TC, Marques AP, Silva SS, Oliveira JM, Mano JF, Castro AG, Reis RL (2007) In vitro evaluation of the behavior of human polymorphonuclear neutrophils in direct contact with chitosan-based membranes. J Biotechnol 132:218–226. doi:10.1016/j.jbiotec.2007.07.497

Saufi SA, Fee CJ (2009) Fractionation of beta-lactoglobulin from whey by mixed matrix membrane ion exchange chromatography. Biotechnol Bioeng 103:138–147. doi:10.1002/bit.22239

Seo T, Ohtake H, Kanbara T, Yonetake K, Iuirna T (1991) Preparation and permeability properties of chitosan membranes having hydrophobic groups. Makromol Chem 192:2447–2461

Silva SS, Luna SM, Gomes ME, Benesch J, Pashkuleva I, Mano JF, Reis RL (2008) Plasma surface modification of chitosan membranes: characterization and preliminary cell response studies. Macromol Biosci 8:568–576. doi:10.1002/mabi.200700264

Singh S, Khulbe KC, Matsuura T, Ramamurthy P (1998) Membrane characterization by solute transport and atomic force microscopy. J Membr Sci 142:111–127

Strathmann H (1981) Membrane separation processes. J Membr Sci 9:121–189

Štulajterová R, Medvecký L (2008) Effect of calcium ions on transformation brushite to hydroxyapatite in aqueous solutions. Colloid Surf A 316:104–109. doi:10.1016/j.colsurfa.2007.08.036

Takeuchi T, Sarashina I, Iijima M, Endo K (2008) In vitro regulation of $CaCO_3$ crystal polymorphism by the highly acidic molluscan shell protein Aspein. FEBS Lett 582:591–596. doi:10.1016/j.febslet.2008.01.026

Tanahashi M, Matsuda T (1997) Surface functional group dependence on apatite formation on self-assembled monolayers in a simulated body fluid. J Biomed Mater Res 34:305–315

Thygesen A, Oddershede J, Lilholt H, Thomsen AB, Ståhl K (2005) On the determination of crystallinity and cellulose content in plant fibres. Cellulose 12:563–576. doi:10.1007/s10570-005-9001-8

Thygesen A, Madsen B, Thomsen AB, Lilholt H (2007) Effect of acidic conditions on interface and strength of cellulose fibres. In: Sørensen BF, Mikkelsen LP, Lilholt H, Goutianos S, Abdul-Mahdi FS (eds) Proceedings of the 28th Risø International Symposium on Materials Science: interface design of polymer matrix composites—mechanics, chemistry, modelling and manufacturing, Risø National Laboratory, Roskilde, Denmark

Toworfe GK, Composto RJ, Shapiro IM, Ducheynea P (2006) Nucleation and growth of calcium phosphate on amine-, carboxyl- and hydroxyl-silane self-assembled monolayers. Biomaterials 27:631–642

Vázquez MI, Lara R, Benavente J (2008) Chemical surface, diffusional, electrical and elastic characterizations of two different dense regenerated cellulose membranes. J Colloid Interf Sci 328:331–337

Vekilov PG, Chernov AA (2002) The physics of protein crystallization. In: Ehrenreich H, Spaepen F (eds) Solid state physics. Academic Press, New York, pp 1–147

Ventura AM, Lahore HMF, Smolko EE, Grasselli M (2008) High-speed protein purification by adsorptive cation-exchange hollow-fiber cartridges. J Membr Sci 321:350–355. doi:10.1016/j.memsci.2008.05.009

Whiteman P (1973) The quantitative measurement of alcian blue-glycosaminoglycan complexes. Biochem J 131:343–350

Xiong X, Duan J, Zou W, He X, Zheng W (2010) A pH-sensitive regenerated cellulose membrane. J Membr Sci 363:96–102. doi:10.1016/j.memsci.2010.07.031

Yang BC, Weng J, Li XD, Zhang XD (1999) The order of calcium and phosphates ion deposition on chemically treated titanium surfaces soaked in aqueous solution. J Biomed Mater Res 47:213–219